JACS
JOURNAL OF THE AMERICAN CHEMICAL SOCIETY
Cite This: J. Am. Chem. Soc. 2018, 140, 16455−16459
Communication
pubs.acs.org/JACS

Three-Dimensional Fully Conjugated Carbaporphyrin Cage

Xian-Sheng Ke,[†] Taeyeon Kim,[‡] Qing He,[†] Vincent M. Lynch,[†] Dongho Kim,[‡] and Jonathan L. Sessler*[†]

[†]Department of Chemistry, The University of Texas at Austin, Austin, Texas 78712-1224, United States
[‡]Department of Chemistry, Yonsei University, Seoul 03722, Korea

* Supporting Information

ABSTRACT: A fully conjugated three-dimensional (3D) expanded carbaporphyrin (2) was prepared in a one-pot procedure that involves a [2+4] condensation reaction between a dibenzo[g,p]chrysene-bearing tetrapyrrole precursor (1) and pentafluorobenzaldehyde, followed by oxidation. Single crystal X-ray diffraction analysis revealed that 2 possesses a cage-like structure consisting of four dipyrromethenes and two bridging dibenzo[g,p]chrysene units. As prepared, 2 is nonaromatic as inferred from UV−vis-NIR and ^{1}H NMR spectroscopy and a near-zero (−1.75) nucleus-independent chemical shift (NICS) value. In contrast, after protonation with trifluoroacetic acid (TFA), the cage gains global aromatic character as inferred from the large negative NICS value (−11.63) and diatropic ring current observed in the anisotropy of the induced current density (ACID) plots, as well as the ca. 2-fold increase in the excited state lifetime. In addition, the size of the cavity increases to ca. 1493 Å^3 upon protonation as deduced from a single crystal X-ray diffraction analysis. To our knowledge, this is the largest carbaporphyrin prepared to date and the first with a fully conjugated 3D cage structure whose size and electronic features may be tuned through protonation.

Topology and conformation are very important not only in natural biological systems but also in synthetic molecules[1]. For instance, biopolymers, including DNA, RNA and proteins, can adopt different knot topologies that associated with specific biochemical activities.[1c] Conjugated molecular systems with ostensibly similar structures can show very different properties. For instance, certain porphyrinoids with figure-eight (double-sided) or a half-twisted (one-sided) topologies can show Hückel- or Möbius-type aromaticity/antiaromaticity, respectively.[2] More broadly, expanded porphyrins have attracted attention because of their conformational flexibility relative to normal tetrapyrrolic porphyrin system and their ability to support unusual topologies.[3] A number of expanded porphyins have been shown to undergo aromaticity switching mediated via conformational changes induced by external stimuli, such as metalation,[4] protonation/deprotonation,[5] temperature changes, and variations in solvent.[5g,6] To date, most experimental work involving conformational and topological switching in the context of porphyrinoids has focused on topographically planar systems. So-called 3D systems, where multiple potential conjugation pathways are constrained within the same nonplanar molecular framework, may allow for further insights. Recently, a number of 3D cage-like porphyrinoids have been reported.[7] However, most of the systems in question are connected by non-conjugated linkages. This necessarily precludes an evaluation of global vs local aromaticity within the enforced 3D structures. Recently, we reported a bicyclic thiophene-based porphyrin analogue system wherein evidence of delocalized electronic structure was seen.[8] Here we report a 3D expanded carbaporphyrin (2) that contains a fully conjugated backbone and whose electronic features may be tuned through protonation.

Carbaporphyrins, porphyrin analogues where one or more nitrogen donor atoms is replaced by a carbon in the central core, have been explored extensively over the last two decades.[9] Carbaporphyrins based on various polycyclic aromatic hydrocarbons (PAHs), including naphthalene,[10] anthracene,[11] phenanthrene,[12] triphenylene,[13] and pyrene[14] are known. Recently, we reported a dibenzo[g,p]chrysene-fused bis-dicarbacorrole (3) derived from a key dibenzo-[g,p]chrysene tetrapyrrole precursor.[15] We have now found that this planar precursor undergoes a face-to-face condensation with an activated aldehyde (C_6F_5CHO) to yield what to our knowledge is the first 3D carbaporphyrin, 2.

The synthesis of 2 is shown in Scheme 1. Briefly, a boron trifluoride etherate-catalyzed [2+4] condensation reaction between the tetrapyrrole precursor 1 and pentafluorobenzaldehyde in dichloromethane (DCM), followed by oxidation

Scheme 1. Synthesis of 3D Expanded Carbaporphyrin 2

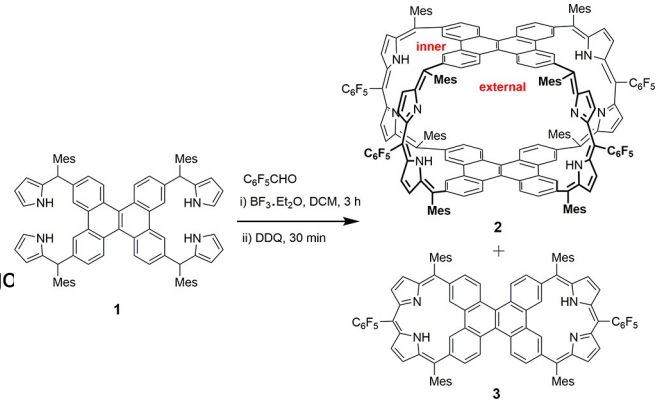

Received: October 16, 2018
Published: November 19, 2018

DOI: 10.1021/jacs.8b11158
J. Am. Chem. Soc. 2018, 140, 16455−16459

with 2,3-dichloro-5,6-dicyano-1,4-benzoquinone (DDQ), the target macrocycle 2 directly. In this reaction, the [1+2] condensation to give the previously reported bis-dicarbacorrole (3)[15a] is more favored, and the yield of 2 is ca. 0.5%. A combination of silica gel chromatography, preparative thin layer chromatography (TLC), and gel permeation chromatography (GPC) allowed the target compound 2 to be isolated as a green solid. Cage 2 was then characterized by ^{1}H, ^{19}F, 2D-correlation spectroscopy (COSY), nuclear Overhauser effect (NOE) NMR, and UV−vis-NIR spectroscopies, high-resolution ESI mass spectrometry, as well as single crystal X-ray diffraction analysis (Figures S1−S8).

Diffraction grade single-crystals of 2 were grown from CH_2Cl_2/n-hexane. The crystal structure confirmed the formation of a [2+4] cage-like condensation product (Figure 1). The two dibenzo[g,p]chrysene moieties are oriented face

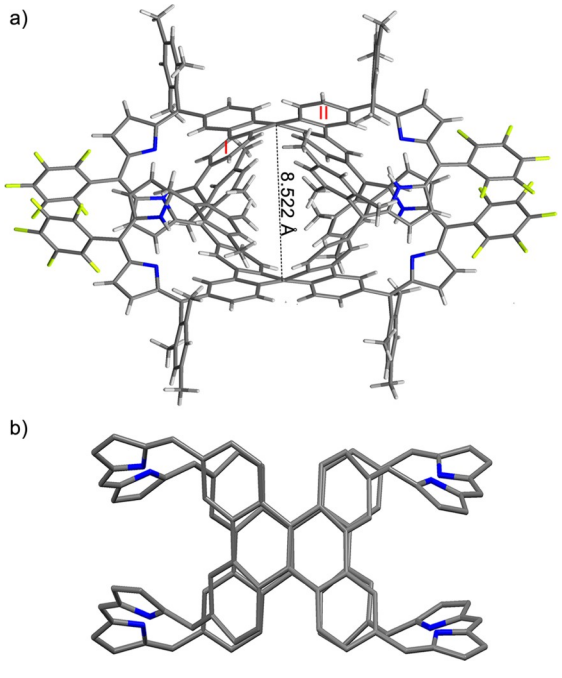

Figure 1. X-ray structure of 2 shown in a stick model; (a) top and (b) side views. Hydrogen atoms and meso-substituents have been omitted for clarity in the side view.

face and are connected by four dipyrromethene units. The bond lengths of the eight carbon−carbon bonds directly linked to the dibenzo[g,p]chrysene backbone are in the range of 1.443−1.488 Å. These values lie close to those expected for carbon−carbon single bonds and are consistent with the corresponding distances found in our previously reported topographically planar bis-dicarbacorrole (3).[15a] The distance between two dibenzo[g,p]chrysene moieties, defined using the centroids of the middle carbon−carbon bond of the constituent chrysene subunits, is ca. 8.522 Å. The dibenzo-[g,p]chrysene bridge in 2 is more distorted than in the corresponding bis-dicarbacorrole (3),[15a] as indicated by an increase in the dihedral angles (35.4° in bis-dicarbacorrole (3) vs 59.9° in cage 2) between the two outer benzene planes (labeled with I and II in Figure 1a). The non-hydrogen atoms in the backbone appear to be sp^2 hybridized as would be expected for a fully conjugated system. Analysis of the structure also reveals that in 2 four meso-mesityl groups are orientated within the inner cavity of the cage (Figure 1) resulting in a small free volume.

The ^{1}H NMR spectrum of 2 was recorded in CD_2Cl_2 and is shown in Figure 2. On the basis of COSY and NOE

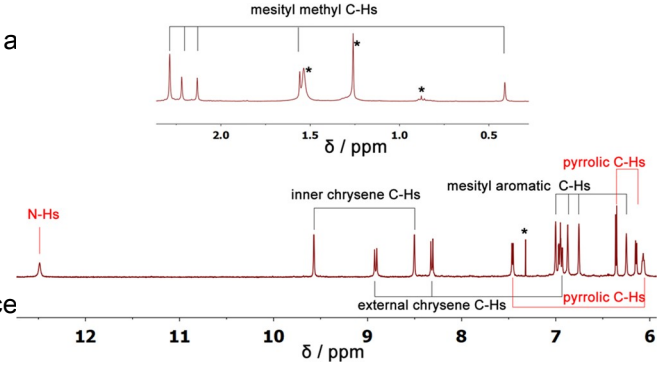

Figure 2. Proton NMR spectrum of cage 2 recorded in CD_2Cl_2. Asterisks indicate residual solvent peaks or impurities.

experiments, the signals of the pyrrolic C−H (6.07−7.46 ppm), inner (8.50−9.57 ppm), and external (6.95−8.91 ppm) chrysene C−H protons can be readily assigned (cf. Figure 2 and Figures S1, S4−S6). The signals of the aromatic meso-mesityl aryl C−H protons are split into four sets of peaks (6.25−7.00 ppm, Figure 2), which is in sharp contrast to the single peak seen for these resonances in the case of the bis-dicarbacorrole (3).[15a] Five signals are seen for the meso-mesityl methyl protons in the case of 2 (0.41−2.29 ppm, Figure 2), whereas only two sets of peaks are seen for these signals in the case of 3.[15a] The increased spectral complexity is taken as an indication that 2 is less symmetric than 3. A upfield shift was seen for some of the meso-mesityl methyl group resonances (as low as 0.41 ppm). Such a finding is consistent with these protons being located within the cage and experiencing a strong shielding effect in accord with the solid state structure shown in Figure 1.

Adding D_2O leads to the disappearance of the pyrrolic N−H proton signal at δ = 12.49 ppm (Figure S7). These N−H resonances are shifted upfield compared to the corresponding signals in 3 (Δ δ = ca. 3.48 ppm).[15a] The average chemical shift difference between the pyrrolic N−H and C−H proton signals (Δδ) was found to be 5.98 ppm, which is less than what was seen in the case of the bis-dicarbacorrole (3)[15a] (10.30 ppm). However, the Δδ seen for 2 is comparable to what was found for a nonaromatic biphenylcorrole[16] (4.64 ppm). We thus conclude that cage 2 is best considered as being nonaromatic.

The UV−vis-NIR spectrum of 2 was recorded in toluene. Two main absorptions bands are seen at 439 and 612 nm, with weaker absorption features over 750−1000 nm spectral region also being observed (Figure 3). The spectrum of 2 matches well with those of benziporphyrin[17] and biphenylcorrole.[16] This provides further support for cage 2 being essentially nonaromatic.

The spectral features of 2 change dramatically when it is treated with acid. For instance, titration with TFA in CD_2Cl_2, causes the meso-mesityl methyl signal at 0.41 ppm in the ^{1}H NMR spectrum to disappear. Moreover, upon treatment with ca. 4 equiv of TFA, all the meso-mesityl methyl signals are seen between ca. 1.77 and 2.42 ppm, a finding taken as evidence of a decreased shielding effect. (Figure S8) Protonation with excess

DOI: 10.1021/jacs.8b11158
J. Am. Chem. Soc. 2018, 140, 16455−16459

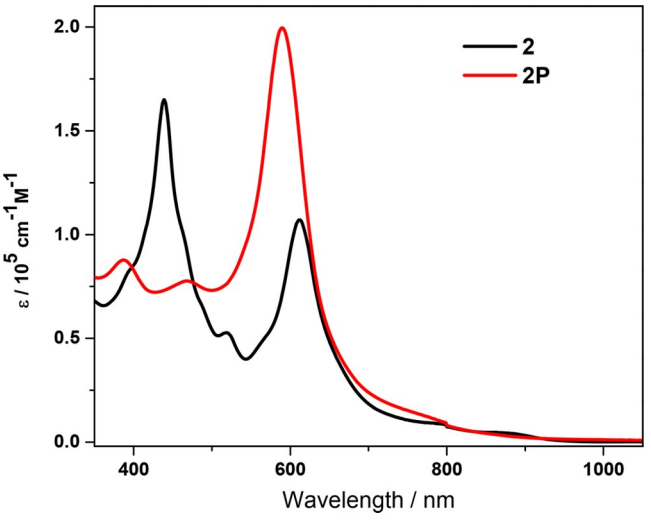

Figure 3. UV−vis-NIR absorption spectra of 2 and its protonated form (2P, generated via the addition of 60 equiv of TFA). Both spectra were recorded in toluene.

TFA also causes the band at 439 nm originally seen in the UV−vis absorption spectrum to disappear, as is replaced by two new low-intensity peaks at ca. 387 and 468 nm (Figure 3). An enhanced absorption at 590 nm is also seen. This latter feature is consistent with increased aromatic character, which leads us to suggest that protonation leads to a change in the electronic structure of 2.

Diffraction grade single-crystals of protonated 2 (2P) were grown from CH_2Cl_2/n-hexane in the presence of excess TFA. Compared with the neutral cage, the distance between two dibenzo[g,p]chrysene moieties increased slightly to 9.293 Å. Inversion of one pyrrole moiety in each dipyrromethene subunit is also seen upon protonation (Figure 4b). More noteworthy is that all the mesityl groups now lie outside of the cage-like inner cavity, a finding that accounts for the decreased shielding effects seen under conditions of solution phase ^{1}H NMR spectral analysis. The fact that the mesityl groups are not in the cavity leads to a more open void, the size of which was calculated to be 143 Å^3 using a virtual rolling probe of 1.5 Å radius (Figure S9). In contrast, almost no void space can be seen in the case of 2 due to the engulfing of the mesityl groups.

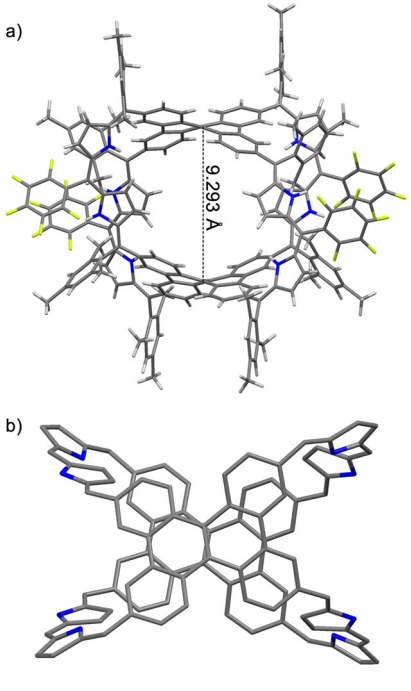

Figure 4. X-ray structure of the protonated form of 2; (a) top and (b) side views. Hydrogen atoms, meso-substituents, TFA anions, and THF molecules have been omitted for clarity in the side view.

In order to probe further the change from nonaromatic to aromatic character that occurs upon protonation, the excited state properties of cage 2 before and after protonation were measured via fs-transient absorption (TA) spectroscopy. Pump pulses (600 nm) were used to probe both the visible and NIR regions. To avoid artifacts (e.g., protonation effects due to halogenated solvent), toluene was used for these measurements. The excited state absorption (ESA) of 2 was characterized by several strong bands at ca. 500, 700, and 1000 nm. In contrast, 2P exhibits relatively weak bands at ca. 650 and 850 nm. The excited state lifetime of 2P (160 ps) proved to be almost 8 times longer than that of 2 (21 ps) (Figure S10). Such an increase is consistent with the proposed increase in aromatic character that occurs upon protonation and a structure that is rigid and stable under conditions of analysis.[5f,18]

Two recognized indicators of aromatic character, namely the nucleus-independent chemical shift (NICS) and anisotropy of the induced current density (AICD), were evaluated via quantum calculations (Figure 5).[19] The NICS(0) values of 2 and 2P were calculated to be −1.75 and −11.63, respectively. The AICD plot of 2 revealed no net overall current. In contrast, that of 2P reveals the presence of diatropic ring current effects, including within the dipyrromethene subunits. These findings proved further support for assigning 2 and 2P as being nonaromatic and aromatic, respectively.

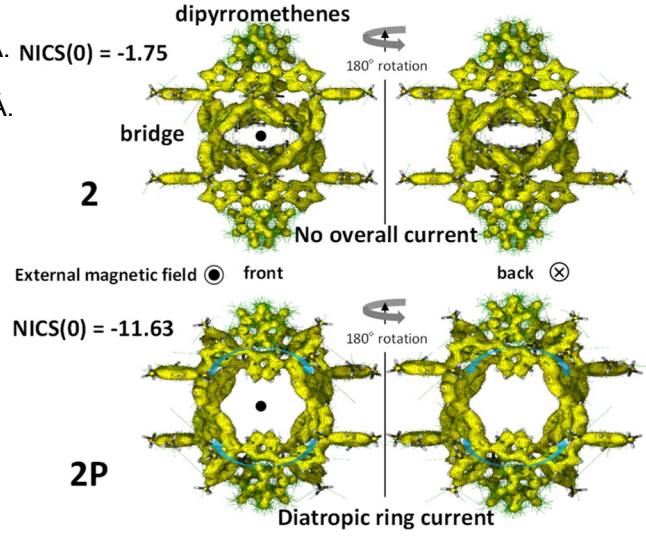

Figure 5. ACID plots of 2 (top) and 2P (bottom). Note that NICS plots viewed from the front and back side of 2 and 2P are presented on the left and right, respectively. NICS(0) were calculated for Bq atoms at the center of each molecule as represented by black dots on the left-hand views.

The bond lengths of the dibenzo[g,p]chrysene bridges and the dipyrromethane linking subunits were also analyzed (Figure S11 and Table S1). Whereas the bond length

DOI: 10.1021/jacs.8b11158
J. Am. Chem. Soc. 2018, 140, 16455−16459

alternations for the dibenzo[g,p]chrysene bridges for 2 and 2P are similar as inferred from the relative standard deviations (RSD) of the bond lengths of 1.8 and 1.7%, respectively, those of dipyrromethene units for 2 and 2P are 3.3 and 2.1%, respectively. Of note is that the latter value comes close to the RSD for the dibenzo[g,p]chrysene bridge in 2P, whereas such a correspondence between the two main portions of the molecule is not seen in the case of 2. On this basis, we conclude that protonation leads to a high degree of conjugation in 2P, as would be expected for a system benefiting from overall aromaticity.

In conclusion, we have prepared and characterized a fully conjugated three-dimensional (3D) expanded carbaporphyrin. The use of a large PAH modified pyrrole precursor, as demonstrated here, provides a synthetic approach to 3D porphyrinoids that complements earlier strategies based on the use of preformed porphyrinoids. The neutral form of 2 displays spectral features consistent with a nonaromatic system. However, an increase in aromatic character is seen upon protonation with TFA. This stimulus-induced switching is made possible in part by the fact that sp^2-hybridized dipyrromethene linkages serve to span the two aromatic dibenzo[g,p]chrysene subunits that make up 2, as well as the choice of a framework that permits effective π-conjugation. Protonation serves to modulate the conformation of the system and open up a small cavity with a discernible free void. Currently, we are targeting new 3D expanded porphyrins with larger internal cavities that might support host−guest interactions within a highly conjugated case, as well as permit further evaluations of the effects of varying global aromaticity.

ASSOCIATED CONTENT

* Supporting Information

The Supporting Information is available free of charge on the ACS Publications website at DOI: 10.1021/jacs.8b11158.

Experimental details and characterization data (PDF)
Data for $C_{192}H_{136}N_8F_{20}^{4+}$, $4C_2F_3O_2^{1-}$, $4C_2F_3O_2H$ (CIF)
Data for $C_{192}H_{132}F_{20}N_8$ (CIF)

AUTHOR INFORMATION

Corresponding Authors
*sessler@cm.utexas.edu
*dongho@yonsei.ac.kr
ORCID
Xian-Sheng Ke: 0000-0002-0562-1039
Qing He: 0000-0003-3117-9587
Dongho Kim: 0000-0001-8668-2644
Jonathan L. Sessler: 0000-0002-9576-1325

Notes

The authors declare no competing financial interest.

ACKNOWLEDGMENTS

The work in Austin was supported by the National Science Foundation (CHE-1807152 to J.L.S.), the Robert A. Welch Foundation (F-0018 to J.L.S.), and the National Institutes of Health (S10 OD021508-01, NMR spectrometer). This research at Yonsei University was supported by the Global Research Laboratory Program (2013K1A1A2A02050183) funded by the Ministry of Science, ICT & Future, Korea (D.K.). The quantum mechanical calculations were supported by the National Institute of Supercomputing and Network (NISN)/Korea Institute of Science and Technology Information (KISTI) with supercomputing resources including technical support (KSC-2018-C3-0008). This research was partially supported by the Graduate School of Yonsei University Research Scholarship Grants in 2000.

REFERENCES

(1) (a) Herges, R. Topology in Chemistry: Designing Möbius Molecules. Chem. Rev. 2006, 106, 4820. (b) Forgan, R. S.; Sauvage, J.-P.; Stoddart, J. F. Chemical Topology: Complex Molecular Knots, Links, and Entanglements. Chem. Rev. 2011, 111, 5434. (c) Lim, N. C. H.; Jackson, S. E. Molecular knots in biology and chemistry. J. Phys.: Condens. Matter 2015, 27, 354101.

(2) (a) Shin, J.-Y.; Kim, K. S.; Yoon, M.-C.; Lim, J. M.; Yoon, Z. S.; Osuka, A.; Kim, D. Aromaticity and photophysical properties of the various topology-controlled expanded porphyrins. Chem. Soc. Rev. 2010, 39, 2751. (b) Sung, Y. M.; Oh, J.; Cha, W.-Y.; Kim, W.; Lim, J. M.; Yoon, M.-C.; Kim, D. Control and Switching of Aromaticity in Various All-Aza-Expanded Porphyrins: Spectroscopic and Theoretical Analyses. Chem. Rev. 2017, 117, 2257.

(3) (a) Yoon, Z. S.; Osuka, A.; Kim, D. Möbius aromaticity and antiaromaticity in expanded porphyrins. Nat. Chem. 2009, 1, 113. (b) Tanaka, T.; Osuka, A. Chemistry of meso-Aryl-Substituted Expanded Porphyrins: Aromaticity and Molecular Twist. Chem. Rev. 2017, 117, 2584.

(4) (a) Park, J. K.; Yoon, Z. S.; Yoon, M.-C.; Kim, K. S.; Mori, S.; Shin, J.-Y.; Osuka, A.; Kim, D. Möbius Aromaticity in N-Fused [24]Pentaphyrin upon Rh(I) Metalation. J. Am. Chem. Soc. 2008, 130, 1824. (b) Tanaka, Y.; Saito, S.; Mori, S.; Aratani, N.; Shinokubo, H.; Shibata, N.; Higuchi, Y.; Yoon, Z. S.; Kim, K. S.; Noh, S. B.; Park, J. K.; Kim, D.; Osuka, A. Metalation of Expanded Porphyrins: A Chemical Trigger Used To Produce Molecular Twisting and Möbius Aromaticity. Angew. Chem., Int. Ed. 2008, 47, 681. (c) Yoneda, T.; Sung, Y. M.; Lim, J. M.; Kim, D.; Osuka, A. PdII Complexes of [44]- and [46]Decaphyrins: The Largest Hückel Aromatic and Antiaromatic, and Möbius Aromatic Macrocycles. Angew. Chem., Int. Ed. 2014, 53, 13169.

(5) (a) Koide, T.; Youfu, K.; Saito, S.; Osuka, A. Multiple conformational changes of β-tetraphenyl meso-hexakis(pentafluorophenyl)substituted [26]- and [28]-hexaphyrins (1.1.1.1.1.1). Chem. Commun. 2009, 6047. (b) Lim, J. M.; Shin, J.-Y.; Tanaka, Y.; Saito, S.; Osuka, A.; Kim, D. Protonated [4n]π and [4n+2]π Octaphyrins: Choose Their Möbius/Hückel Aromatic Topology. J. Am. Chem. Soc. 2010, 132, 3105. (c) Ishida, S.-i.; Higashino, T.; Mori, S.; Mori, H.; Aratani, N.; Tanaka, T.; Lim, J. M.; Kim, D.; Osuka, A. Diprotonated [28]Hexaphyrins (1.1.1.1.1.1): Triangular Antiaromatic Macrocycles. Angew. Chem., Int. Ed. 2014, 53, 3427. (d) Cha, W.-Y.; Yoneda, T.; Lee, S.; Lim, J. M.; Osuka, A.; Kim, D. Deprotonation induced formation of Möbius aromatic [32]-heptaphyrins. Chem. Commun. 2014, 50, 548. (e) Naoda, K.; Osuka, A. Structural and Aromaticity Control of [34]-Octaphyrin (1.1.1.0.1.1.1.0) by Protonation and Deprotonation. Asian J. Org. Chem. 2017, 6, 1205. (f) Oh, J.; Mori, H.; Sung, Y. M.; Kim, W.; Osuka, A.; Kim, D. Switchable π-electronic network of bis(α-oligothienyl)-substituted hexaphyrins between helical versus rectangular circuit. Chem. Sci. 2016, 7, 2239. (g) Mallick, A.; Oh, J.; Majewski, M. A.; Stępień, M.; Kim, D.; Rath, H. Protonation Dependent Topological Dichotomy of Core Modified Hexaphyrins: Synthesis, Characterization, and Excited State Dynamics. J. Org. Chem. 2017, 82, 556.

(6) (a) Kim, K. S.; Yoon, Z. S.; Ricks, A. B.; Shin, J.-Y.; Mori, S.; Sankar, J.; Saito, S.; Jung, Y. M.; Wasielewski, M. R.; Osuka, A.; Kim, D. Temperature-Dependent Conformational Change of meso-Hexakis(pentafluorophenyl) [28]Hexaphyrins (1.1.1.1.1.1) into Möbius Structures. J. Phys. Chem. A 2009, 113, 4498. (b) Yoon, M.-C.; Kim, P.; Yoo, H.; Shimizu, S.; Koide, T.; Tokuji, S.; Saito, S.; Osuka, A.; Kim, D. Solvent- and Temperature-Dependent Conformational Changes between Hückel Antiaromatic and Möbius Aromatic Species

DOI: 10.1021/jacs.8b11158
J. Am. Chem. Soc. 2018, 140, 16455−16459

in meso-Trifluoromethyl Substituted [28]Hexaphyrins. J. Phys. Chem. B 2011, 115, 14928.
(7) (a) Durot, S.; Taesch, J.; Heitz, V. Multiporphyrinic Cages: Architectures and Functions. Chem. Rev. 2014, 114, 8542 and references cited therein. (b) Hong, S.; Rohman, M. R.; Jia, J.; Kim, Y.; Moon, D.; Kim, Y.; Ko, Y. H.; Lee, E.; Kim, K. Porphyrin Boxes: Rationally Designed Porous Organic Cages. Angew. Chem., Int. Ed. 2015, 54, 13241. (c) Zhang, D.; Ronson, T. K.; Nitschke, J. R. Functional Capsules via Subcomponent Self-Assembly. Acc. Chem. Res. 2018, 51, 2423. (d) Shi, Y.; Cai, K.; Xiao, H.; Liu, Z.; Zhou, J.; Shen, D.; Qiu, Y.; Guo, Q.; Stern, C.; Wasielewski, M. R.; Diederich, F.; Goddard, W. A.; Stoddart, J. F. Selective Extraction of C_{70} by a Tetragonal Prismatic Porphyrin Cage. J. Am. Chem. Soc. 2018, 140, 13835.
(8) Cha, W.-Y.; Kim, T.; Ghosh, A.; Zhang, Z.; Ke, X.-S.; Ali, R.; Lynch, V. M.; Jung, J.; Kim, W.; Lee, S.; Fukuzumi, S.; Park, J. S.; Sessler, J. L.; Chandrashekar, T. K.; Kim, D. Bicyclic Baird-type aromaticity. Nat. Chem. 2017, 9, 1243.
(9) Lash, T. D. Carbaporphyrinoid Systems. Chem. Rev. 2017, 117, 2313.
(10) (a) Lash, T. D.; Young, A. M.; Rasmussen, J. M.; Ferrence, G. M. Naphthiporphyrins. J. Org. Chem. 2011, 76, 5636. (b) Szyszko, B.; Pacholska-Dudziak, E.; Latos-Grażyński, L. Incorporation of the 1,5-Naphthalene Subunit into Heteroporphyrin Structure: Toward Helical Aceneporphyrinoids. J. Org. Chem. 2013, 78, 5090. (c) Hong, J.-H.; Aslam, A. S.; Ishida, M.; Mori, S.; Furuta, H.; Cho, D.-G. 2-(Naphthalen-1-yl)thiophene as a New Motif for Porphyrinoids: Meso-Fused Carbaporphyrin. J. Am. Chem. Soc. 2016, 138, 4992.
(11) (a) Szyszko, B.; Latos-Grażyński, L.; Szterenberg, L. Toward aceneporphyrinoids: synthesis and transformations of palladium(ii) meso-anthriporphyrin. Chem. Commun. 2012, 48, 5004. (b) Sung, Y. M.; Szyszko, B.; Mysliborski, R.; Stepień, M.; Oh, J.; Son, M.; Latos-Grażyński, L.; Kim, D. The effect of π-conjugation in the macrocyclic ring on the photophysical properties of a series of thiaaceneporphyrinoids. Chem. Commun. 2014, 50, 8367. (c) Aslam, A. S.; Hong, J.-H.; Shin, J.-H.; Cho, D.-G. Synthesis of a Phlorin from a Meso-Fused Anthriporphyrin by a Diels−Alder Strategy. Angew. Chem., Int. Ed. 2017, 56, 16247.
(12) (a) Szyszko, B.; Bialonska, A.; Szterenberg, L.; Latos-Grażyński, L. Phenanthriporphyrin: An Antiaromatic Aceneporphyrinoid as Ligand for a Hypervalent Organophosphorus(V) Moiety. Angew. Chem., Int. Ed. 2015, 54, 4932. (b) Szyszko, B.; Małecki, M.; Berlicka, A.; Białek, M. J.; Białońska, A.; Kupietz, K.; Pacholska-Dudziak, E.; Latos-Grażyński, L. Incorporation of a Phenanthrene Subunit into a Sapphyrin Framework: Synthesis of Expanded Aceneporphyrinoids. Chem. - Eur. J. 2016, 22, 7602.
(13) Gopee, H.; Kong, X.; He, Z.; Chambrier, I.; Hughes, D. L.; Tizzard, G. J.; Coles, S. J.; Cammidge, A. N. Expanded Porphyrin-like Structures Based on Twinned Triphenylenes. Org. Chem. 2013, 78, 9505.
(14) Gao, R.; AbuSalim, D. I.; Lash, T. D. Pyreniporphyrins: Porphyrin Analogues That Incorporate a Polycyclic Aromatic Hydrocarbon Subunit within the Macrocyclic Framework. J. Org. Chem. 2017, 82, 6680.
(15) (a) Ke, X.-S.; Hong, Y.; Tu, P.; He, Q.; Lynch, V. M.; Kim, D.; Sessler, J. L. Hetero Cu(III)−Pd(II) Complex of a Dibenzo[g,p]-chrysene-Fused Bis-dicarbacorrole with Stable Organic Radical Character. J. Am. Chem. Soc. 2017, 139, 15232. (b) Ke, X.-S.; Hong, Y.; Lynch, V. M.; Kim, D.; Sessler, J. L. Metal-Stabilized Quinoidal Dibenzo[g,p]chrysene-Fused Bis-dicarbacorrole System. J. Am. Chem. Soc. 2018, 140, 7579.
(16) Adinarayana, B.; Thomas, A. P.; Suresh, C. H.; Srinivasan, A. A 6,11,16-Triarylbiphenylcorrole with an adj-CCNN Core: Stabilization of an Organocopper(III) Complex. Angew. Chem., Int. Ed. 2015, 54, 10478.
(17) Stępień, M.; Latos-Grażyński, L. Tetraphenylbenziporphyrin: A Ligand for Organometallic Chemistry. Chem. - Eur. J. 2001, 7, 5113.
(18) Cha, W.-Y.; Lim, J. M.; Yoon, M.-C.; Sung, Y. M.; Lee, B. S.; Katsumata, S.; Suzuki, M.; Mori, H.; Ikawa, Y.; Furuta, H.; Osuka, A.; Kim, D. Deprotonation-Induced Aromaticity Enhancement and New Conjugated Networks in meso-Hexakis(pentafluorophenyl)[26]-hexaphyrin. Chem. - Eur. J. 2012, 18, 15838.
(19) Sung, Y. M.; Yoon, M.-C.; Lim, J. M.; Rath, H.; Naoda, K.; Osuka, A.; Kim, D. Reversal of Hückel (anti)aromaticity in the lowest triplet states of hexaphyrins and spectroscopic evidence for Baird rule. Nat. Chem. 2015, 7, 418.

DOI: 10.1021/jacs.8b11158
J. Am. Chem. Soc. 2018, 140, 16455−16459